Journal pre-proof

DOI: 10.1016/j.cell.2020.02.052

SARS-CoV-2 cell entry depends on ACE2 and TMPRSS2 and is blocked by a clinically-proven protease inhibitor

Markus Hoffmann,[1,13*] Hannah Kleine-Weber,[1,2,13], Simon Schroeder,[3,4] Nadine Krüger,[5,6] Tanja Herrler,[7] Sandra Erichsen,[8,9] Tobias S. Schiergens[10], Georg Herrler,[5] Nai-Huei Wu,[5] Andreas Nitsche,[11] Marcel A. Müller,[3,4,12] Christian Drosten,[3,4] Stefan Pöhlmann[1,2,14*]

[1]Infection Biology Unit, German Primate Center – Leibniz Institute for Primate Research, Göttingen, Germany

[2]Faculty of Biology and Psychology, University Göttingen, Göttingen, Germany

[3]Charité-Universitätsmedizin Berlin, corporate member of Freie Universität Berlin, Humboldt-Universität zu Berlin, and Berlin Institute of Health, Institute of Virology, Berlin, Germany

[4]German Centre for Infection Research, associated partner Charité, Berlin, Germany

[5]Institute of Virology, University of Veterinary Medicine Hannover, Hannover, Germany.

[6]Research Center for Emerging Infections and Zoonoses, University of Veterinary Medicine Hannover, Hannover, Germany

[7]BG Unfallklinik Murnau, Murnau, Germany

[8]Institute for Biomechanics, BG Unfallklinik Murnau, Murnau, Germany

[9]Institute for Biomechanics, Paracelsus Medical University Salzburg, Salzburg, Austria

[10] Biobank of the Department of General, Visceral, and Transplant Surgery, Ludwig-Maximilians-University Munich, Munich, Germany

[11]Robert Koch Institute, ZBS 1 Highly Pathogenic Viruses, WHO Collaborating Centre for Emerging Infections and Biological Threats, Berlin, Germany

[12]Martsinovsky Institute of Medical Parasitology, Tropical and Vector Borne Diseases, Sechenov University, Moscow, Russia

[13]These authors contributed equally

[14]Lead contact

[*]Correspondence: mhoffmann@dpz.eu (M.H.), spoehlmann@dpz.eu (S.P.)

SUMMARY

The recent emergence of the novel, pathogenic SARS-coronavirus 2 (SARS-CoV-2) in China and its rapid national and international spread pose a global health emergency. Cell entry of coronaviruses depends on binding of the viral spike (S) proteins to cellular receptors and on S protein priming by host cell proteases. Unravelling which cellular factors are used by SARS-CoV-2 for entry might provide insights into viral transmission and reveal therapeutic targets. Here, we demonstrate that SARS-CoV-2 uses the SARS-CoV receptor, ACE2, for entry and the serine protease TMPRSS2 for S protein priming. A TMPRSS2 inhibitor approved for clinical use blocked entry and might constitute a treatment option. Finally, we show that the sera from convalescent SARS patients cross-neutralized SARS-2-S-driven entry. Our results reveal important commonalities between SARS-CoV-2 and SARS-CoV infection and identify a potential target for antiviral intervention.

INTRODUCTION

Several members of the family *Coronaviridae* constantly circulate in the human population and usually cause mild respiratory disease (Corman et al., 2019). In contrast, the severe acute respiratory syndrome coronavirus (SARS-CoV) and the Middle East respiratory syndrome coronavirus (MERS-CoV) are transmitted from animals to humans and cause severe respiratory diseases in afflicted individuals, SARS and MERS, respectively (Fehr et al., 2017). SARS emerged in 2002 in Guangdong province, China, and its subsequent global spread was associated with 8096 cases and 774 deaths (de Wit et al., 2016; WHO, 2004). Chinese horseshoe bats serve as natural reservoir hosts for SARS-CoV (Lau et al., 2005; Li et al., 2005a). Human transmission was facilitated by intermediate hosts like civet cats and raccoon dogs, which are frequently sold as food sources in Chinese wet markets (Guan et al., 2003). At present, no specific antivirals or approved vaccines are available to combat SARS, and the SARS pandemic in 2002/2003 was finally stopped by conventional control measures, including travel restrictions and patient isolation.

In December 2019 a new infectious respiratory disease emerged in Wuhan, Hubei province, China (Huang et al., 2020; Wang et al., 2020; Zhu et al., 2020). An initial cluster of infections was linked to Huanan seafood market, potentially due to animal contact. Subsequently, human-to-human transmission occurred (Chan et al., 2020) and the disease, now termed coronavirus disease 19 (COVID-19) rapidly spread within China. A novel coronavirus, SARS-CoV-2, which is closely related to SARS-CoV, was detected in patients and is believed to be the etiologic agent of the new lung disease (Zhu et al., 2020). On February 12, 2020, at total of 44,730 laboratory confirmed infections were reported in China, including 8204 severe cases and 1114 deaths (WHO, 2020). Infections were also detected in 24 countries outside China and were associated with international travel. At present, it is unknown whether the sequence similarities

between SARS-CoV-2 and SARS-CoV translate into similar biological properties, including pandemic potential (Munster et al., 2020).

The spike (S) protein of coronaviruses facilitates viral entry into target cells. Entry depends on binding of the surface unit, S1, of the S protein to a cellular receptor, which facilitates viral attachment to the surface of target cells. In addition, entry requires S protein priming by cellular proteases, which entails S protein cleavage at the S1/S2 and the S2' site and allows fusion of viral and cellular membranes, a process driven by the S2 subunit (Figure 1A). SARS-S engages angiotensin-converting enzyme 2 (ACE2) as entry receptor (Li et al., 2003) and employs the cellular serine protease TMPRSS2 for S protein priming (Glowacka et al., 2011; Matsuyama et al., 2010; Shulla et al., 2011). The SARS-S/ACE2 interface has been elucidated at the atomic level and the efficiency of ACE2 usage was found to be a key determinant of SARS-CoV transmissibility (Li et al., 2005a; Li et al., 2005b). SARS-S und SARS-2-S share ~76% amino acid identity. However, it is unknown whether SARS-2-S like SARS-S employs ACE2 and TMPRSS2 for host cell entry.

RESULTS

Evidence for efficient proteolytic processing of SARS-2-S

The goal of our study was to obtain insights into how SARS-2-S facilitates viral entry into target cells and how this process can be blocked. For this, we first asked whether SARS-2-S is robustly expressed in a human cell line, 293T, commonly used for experimentation due to its high transfectability. Moreover, we analyzed whether there is evidence for proteolytic processing of the S protein since certain coronavirus S proteins are cleaved by host cell proteases at the S1/S2 cleavage site in infected cells (Figure 1A). Immunoblot analysis of 293T cells expressing SARS-2-S protein with a C-terminal antigenic tag revealed a band with a molecular weight expected for unprocessed S protein (S0) (Figure 1B). A band with a size expected for the S2 subunit of the S protein was also observed in cells and, more prominently, in vesicular stomatitis virus (VSV) particles bearing SARS-2-S (Figure 1B). In contrast, an S2 signal was largely absent in cells and particles expressing SARS-S (Figure 1B), as previously documented (Glowacka et al., 2011; Hofmann et al., 2004b). These results suggest efficient proteolytic processing of SARS-2-S in human cells, in keeping with the presence of several arginine residues at the S1/S2 cleavage site of SARS-2-S but not SARS-S (Figure 1A). In contrast, the S2' cleavage site of SARS-2-S was similar to that of SARS-S.

SARS-2-S and SARS-S mediate entry into a similar spectrum of cell lines

Replication-defective VSV particles bearing coronavirus S proteins faithfully reflect key aspects of coronavirus host cell entry (Kleine-Weber et al., 2019). We employed VSV pseudotypes bearing SARS-2-S to study cell entry of SARS-CoV-2. Both SARS-2-S and SARS-S were robustly incorporated into VSV particles (Figure 1B), allowing a meaningful side-by-side

144 comparison, although, formally, comparable particle incorporation of the S1 subunit remains to
145 be demonstrated. We first asked which cell lines were susceptible to SARS-2-S-driven entry,
146 using a panel of well characterized cell lines of human and animal origin, respectively. All cell
147 lines were readily susceptible to entry driven by the glycoprotein of the pantropic VSV (VSV-G)
148 (Figure 1C and Figure S1), as expected. Most human cell lines and the animal cell lines Vero and
149 MDCKII were also susceptible to entry driven by SARS-S (Figure 1C). Moreover, SARS-2-S
150 facilitated entry into an identical spectrum of cell lines as SARS-S (Figure 1C), suggesting
151 similarities in choice of entry receptors.
152
153 **SARS-CoV-2 employs the SARS-CoV receptor for host cell entry**
154 In order to elucidate why SARS-S and SARS-2-S mediated entry into the same cell lines, we next
155 determined whether SARS-2-S harbors amino acid residues required for interaction with the
156 SARS-S entry receptor ACE2. Sequence analysis revealed that SARS-CoV-2 clusters with
157 SARS-CoV-related viruses from bats (SARSr-CoV), of which some but not all can use ACE2 for
158 host cell entry (Figure 2A and Figure S2). Analysis of the receptor binding motif (RBM), a
159 portion of the receptor binding domain (RBD) that makes contact with ACE2 (Li et al., 2005a),
160 revealed that most amino acid residues essential for ACE2 binding by SARS-S were conserved in
161 SARS-2-S (Figure 2B). In contrast, most of these residues were absent from S proteins of
162 SARSr-CoV previously found not to use ACE2 for entry (Figure 2B) (Ge et al., 2013; Hoffmann
163 et al., 2013; Menachery et al., 2019). In agreement with these findings, directed expression of
164 human and bat (*Rhinolophus alcyone*) ACE2 but not human DPP4, the entry receptor used by
165 MERS-CoV (Raj et al., 2013), or human APN, the entry receptor used by HCoV-229E (Yeager et
166 al., 1992), allowed SARS-2-S- and SARS-S-driven entry into otherwise non-susceptible BHK-21
167 cells (Figure 3A). Moreover, antiserum raised against human ACE2 blocked SARS-S- and

SARS-2-S- but not VSV-G- or MERS-S-driven entry (Figure 3B). Finally, authentic SARS-CoV-2 infected BHK-21 cells transfected to express ACE2 cells but not parental BHK-21 cells with high efficiency (Figure 3C), indicating that SARS-2-S, like SARS-S, uses ACE2 for cellular entry.

The cellular serine protease TMPRSS2 primes SARS-2-S for entry and a serine protease inhibitor blocks SARS-CoV-2 infection of lung cells

We next investigated protease dependence of SARS-CoV-2 entry. SARS-CoV can use the endosomal cysteine proteases cathepsin B and L (CatB/L) (Simmons et al., 2005) and the serine protease TMPRSS2 (Glowacka et al., 2011; Matsuyama et al., 2010; Shulla et al., 2011) for S protein priming in cell lines, and inhibition of both proteases is required for robust blockade of viral entry (Kawase et al., 2012). However, only TMPRSS2 activity is essential for viral spread and pathogenesis in the infected host while CatB/L activity is dispensable (Iwata-Yoshikawa et al., 2019; Shirato et al., 2017; Shirato et al., 2018; Zhou et al., 2015).

In order to determine whether SARS-CoV-2 can use CatB/L for cell entry, we initially employed ammonium chloride, which elevates endosomal pH and thereby blocks CatB/L activity. 293T cells (TMPRSS2$^-$, transfected to express ACE2 for robust S protein-driven entry) and Caco-2 cells (TMPRSS2$^+$) were used as targets. Ammonium chloride blocked VSV-G-dependent entry into both cell lines while entry driven by Nipah virus F and G proteins was not affected (Figure S3 panel A and data not shown), in keeping with Nipah virus but not VSV being able to fuse directly with the plasma membrane (Bossart et al., 2002). Ammonium chloride treatment strongly inhibited SARS-2-S- and SARS-S-driven entry into TMPRSS2$^-$ 293T cells (Figure S3 panel A), suggesting CatB/L dependence. Inhibition of entry into TMPRSS2$^+$ Caco-2 cells was less efficient as compared to 293T cells (Figure S3 panel A), which would be

compatible with SARS-2-S priming by TMPRSS2 in Caco-2 cells. Indeed, the clinically-proven serine protease inhibitor camostat mesylate, which is active against TMPRSS2 (Kawase et al., 2012), partially blocked SARS-2-S-driven entry into Caco-2 (Figure S3 panel B) and Vero-TMPRSS2 cells (Figure 4A). Full inhibition was attained when camostat mesylate and E-64d, an inhibitor of CatB/L, were added (Figure S3 panel B and Figure 4A), indicating that SARS-2-S can use both CatB/L as well as TMPRSS2 for priming in these cell lines. In contrast, camostat mesylate did not interfere with SARS-2-S-driven entry into the TMPRSS2$^-$ cell lines 293T (Figure S3 panel B) and Vero (Figure 4A) which was efficiently blocked by E-64d and thus CatB/L-dependent. Moreover, directed expression of TMPRSS2 rescued SARS-2-S-driven entry from inhibition by E-64d (Figure 4B), confirming that SARS-2-S can employ TMPRSS2 for S protein priming.

We next analyzed whether TMPRSS2 usage is required for SARS-CoV-2 infection of lung cells. Indeed, camostat mesylate significantly reduced MERS-S-, SARS-S- and SARS-2-S- but not VSV-G-driven entry into the lung cell line Calu-3 (Figure 4C) and exerted no unwanted cytotoxic effects (Figure S3 panel C). Similarly, camostat mesylate treatment significantly reduced Calu-3 infection with authentic SARS-CoV-2 (Figure 4D). Finally, camostat mesylate treatment inhibited SARS-S- and SARS-2-S- but not VSV-G-driven entry into primary human lung cells (Figure 4E). Collectively, SARS-CoV-2 can use TMPRSS2 for S protein priming and camostat mesylate, an inhibitor of TMPRSS2, blocks SARS-CoV-2 infection of lung cells.

Evidence that antibodies raised against SARS-CoV will cross-neutralize SARS-CoV-2

Convalescent SARS patients exhibit a neutralizing antibody response directed against the viral S protein (Liu et al., 2006). We investigated whether such antibodies block SARS-2-S-driven entry. Four sera obtained from three convalescent SARS patients inhibited SARS-S- but

not VSV-G-driven entry in a concentration dependent manner (Figure 5). In addition, these sera also reduced SARS-2-S-driven entry, although with lower efficiency as compared to SARS-S (Figure 5). Similarly, rabbit sera raised against the S1 subunit of SARS-S reduced both SARS-S- and SARS-2-S-driven entry with high efficiency and again inhibition of SARS-S-driven entry was more efficient. Thus, antibody responses raised against SARS-S during infection or vaccination might offer some level of protection against SARS-CoV-2 infection.

DISCUSSION

The present study provides evidence that host cell entry of SARS-CoV-2 depends on the SARS-CoV receptor ACE2 and can be blocked by a clinically-proven inhibitor of the cellular serine protease TMPRSS2, which is employed by SARS-CoV-2 for S protein priming. Moreover, it suggests that antibody responses raised against SARS-CoV could at least partially protect against SARS-CoV-2 infection. These results have important implications for our understanding of SARS-CoV-2 transmissibility and pathogenesis and reveal a target for therapeutic intervention.

The finding that SARS-2-S exploits ACE2 for entry, which was also reported by Zhou and colleagues (Zhou et al., 2020) while the present manuscript was in revision, suggests that the virus might target a similar spectrum of cells as SARS-CoV. In the lung, SARS-CoV infects mainly pneumocytes and macrophages (Shieh et al., 2005). However, ACE2 expression is not limited to the lung and extrapulmonary spread of SARS-CoV in $ACE2^+$ tissues was observed (Ding et al., 2004; Gu et al., 2005; Hamming et al., 2004). The same can be expected for SARS-CoV-2, although affinity of SARS-S and SARS-2-S for ACE2 remains to be compared. It has been suggested that the modest ACE2 expression in the upper respiratory tract (Bertram et al., 2012; Hamming et al., 2004) might limit SARS-CoV transmissibility. In the light of the potentially increased transmissibility of SARS-CoV-2 relative to SARS-CoV one may speculate that the new virus might exploit cellular attachment-promoting factors with higher efficiency as SARS-CoV to ensure robust infection of $ACE2^+$ cells in the upper respiratory tract. This could comprise binding to cellular glycans, a function ascribed to the S1 domain of certain coronaviruses (Li et al., 2017; Park et al., 2019). Finally, it should be noted that ACE2 expression protects from lung injury and is downregulated by SARS-S (Haga et al., 2008; Imai et al., 2005; Kuba et al., 2005), which might promote SARS. It will thus be interesting to determine whether SARS-CoV-2 also interferes with ACE2 expression.

Priming of coronavirus S proteins by host cell proteases is essential for viral entry into cells and encompasses S protein cleavage at the S1/S2 and the S2' sites. The S1/S2 cleavage site of SARS-2-S harbors several arginine residues (multibasic), which indicates high cleavability. Indeed, SARS-2-S was efficiently cleaved in cells and cleaved S protein was incorporated into VSV particles. Notably, the cleavage site sequence can determine the zoonotic potential of coronaviruses (Menachery et al., 2019; Yang et al., 2014; Yang et al., 2015) and a multibasic cleavage site was not present in RaTG13, the coronavirus most closely related to SARS-CoV-2. It will thus be interesting to determine whether the presence of a multibasic cleavage site is required for SARS-CoV-2 entry into human cells and how this cleavage site was acquired.

The S proteins of SARS-CoV can use the endosomal cysteine proteases CatB/L for S protein priming in TMPRSS2$^-$ cells (Simmons et al., 2005). However, S protein priming by TMPRSS2 but not CatB/L is essential for viral entry into primary target cells and for viral spread in the infected host (Iwata-Yoshikawa et al., 2019; Kawase et al., 2012; Zhou et al., 2015). The present study indicates that SARS-CoV-2 spread also depends on TMPRSS2 activity, although we note that SARS-CoV-S2 infection of Calu-3 cells was inhibited but not abrogated by camostat mesylate, likely reflecting residual S protein priming by CatB/L. One can speculate that furin-mediated precleavage at the S1/S2 site in infected cells might promote subsequent TMPRSS2-dependent entry into target cells, as reported for MERS-CoV (Kleine-Weber et al., 2018; Park et al., 2016). Collectively, our present findings and previous work highlight TMPRSS2 as a host cell factor which is critical for spread of several clinically relevant viruses, including influenza A viruses and coronaviruses (Gierer et al., 2013; Glowacka et al., 2011; Iwata-Yoshikawa et al., 2019; Kawase et al., 2012; Matsuyama et al., 2010; Shulla et al., 2011; Zhou et al., 2015). In contrast, TMPRSS2 is dispensable for development and homeostasis (Kim et al., 2006) and thus constitutes an attractive drug target. In this context, it is noteworthy that the serine protease

inhibitor camostat mesylate, which blocks TMPRSS2 activity (Kawase et al., 2012; Zhou et al., 2015), has been approved in Japan for human use, although for an unrelated indication. This compound or related ones with potentially increased antiviral activity (Yamamoto et al., 2016) could thus be considered for off-label treatment of SARS-CoV-2 infected patients.

Convalescent SARS patients exhibit a neutralizing antibody response that can be detected even 24 months after infection (Liu et al., 2006) and that is largely directed against the S protein. Moreover, experimental SARS vaccines, including recombinant S protein (He et al., 2006) and inactivated virus (Lin et al., 2007) induce neutralizing antibody responses. Although confirmation with infectious virus is pending, our results indicate that neutralizing antibody responses raised against SARS-S could offer some protection against SARS-CoV-2 infection, which may have implications for outbreak control.

In sum, this study provided key insights into the first step of SARS-CoV-2 infection, viral entry into cells, and defined potential targets for antiviral intervention.

ACKNOWLEDGEMENTS

We thank Heike Hofmann-Winkler for discussion, (Andrea Maisner for Nipah F and G expression plasmids and Roberto Cattaneo for plasmid pCG1. We acknowledge the support of the non-profit foundation HTCR, which holds human tissue on trust, making it broadly available for research on an ethical and legal basis. We gratefully acknowledge the authors, the originating and submitting laboratories for their sequence and metadata shared through GISAID, on which this research is based. This work was supported by BMBF (RAPID Consortium, 01KI1723D and 01KI1723A to C.D. and S.P.) and German Research Foundation (DFG) (WU 929/1-1 to N.-H. W.).

AUTHOR CONTRIBUTIONS

Conceptualization, M.H. and S.P.; Formal analysis, M.H., H.-K.W., M.A.M, S.P.; Investigation, M.H., H.K.-W, S.S., N.K., T.H., N.-H. W. and M.A.M.; Resources, T.H., S.E., T.S.S., G.H., A.N., M.A.M. and C.D.; Writing – Original Draft, M.H. and S.P.; Writing -Review & Editing, all authors; Funding acquisition, S.P., N.-H.W. and C.D.

DECLARATION OF INTEREST

The authors declare not competing interests

FIGURE LEGENDS

Figure 1. SARS-2-S and SARS-S facilitate entry into a similar panel of mammalian cell lines

(A) Schematic illustration of SARS-S including functional domains (RBD = receptor binding domain, RBM = receptor binding motif, TD = transmembrane domain) and proteolytic cleavage sites (S1/S2, S2‘). Amino acid sequences around the two protease recognition sites (red) are indicated for SARS-S and SARS-2-S (asterisks indicate conserved residues). Arrow heads indicate the cleavage site.

(B) Analysis of SARS-2-S expression (upper panel) and pseudotype incorporation (lower panel) by Western blot using an antibody directed against the C-terminal HA tag added to the viral S proteins analyzed. Shown are representative blots from three experiments. ß-Actin (cell lysates) and VSV-M (particles) served as loading controls. Black arrow heads indicate bands corresponding to uncleaved S proteins (S0) while grey arrow heads indicate bands corresponding to the S2 subunit.

(C) Cell lines of human and animal origin were inoculated with pseudotyped VSV harboring VSV-G, SARS-S or SARS-2-S. At 16 h postinoculation, pseudotype entry was analyzed by determining luciferase activity in cell lysates. Signals obtained for particles bearing no envelope protein were used for normalization. The average of three independent experiments is shown. Error bars indicate SEM. Unprocessed data from a single experiment are presented in Figure S1.

Figure 2. SARS-2-S harbors amino acid residues critical for ACE2 binding

(A) The S protein of SARS-CoV-2 clusters phylogenetically with S proteins of known bat-associated betacoronaviruses (see figure S2 for more details).

(B) Alignment of the receptor binding motif of SARS-S with corresponding sequences of bat-associated betacoronavirus S proteins, which are able or unable to use ACE2 as cellular receptor reveals that SARS-CoV-2 possesses crucial amino acid residues for ACE2 binding.

Figure 3. SARS-2-S utilizes ACE2 as cellular receptor

(A) BHK-21 cells transiently expressing ACE2 of human or bat origin, human APN or human DPP4 were inoculated with pseudotyped VSV harboring VSV-G, SARS-S, SARS-2-S, MERS-S or 229E-S. At 16 h postinoculation, pseudotype entry was analyzed (normalization against particles without viral envelope protein).

(B) Untreated Vero cells as well as Vero cells pre-incubated with 2 or 20 µg/ml anti-ACE2 antibody or unrelated control antibody (anti-DC-SIGN, 20 µg/ml) were inoculated with pseudotyped VSV harboring VSV-G, SARS-S, SARS-2-S or MERS-S. At 16 h postinoculation, pseudotype entry was analyzed (normalization against untreated cells).

(C) BHK-21 cells transfected with ACE2-encoding plasmid or control transfected with DsRed encoding plasmid were infected with SARS-CoV-2, washed and genome equivalents in culture supernatants determined by quantitative RT-PCR.

The average of three independent experiments conducted with triplicate samples is shown in panels A-C. Error bars indicate SEM. Statistical significance was tested by two-way ANOVA with Dunnett posttest. Cells transfected with empty vector served as reference in panel A while cells that were not treated with antibody served as reference in panel B.

Figure 4. SARS-2-S employs TMPRSS2 for S protein priming

(A) Importance of activity of CatB/L or TMPRSS2 for host cell entry of SARS-CoV-2 was evaluated by adding inhibitors to target cells prior to transduction. E-64d and camostat mesylate

block the activity of CatB/L and TMPRSS2, respectively (additional data for 293T cells transiently expressing ACE2 and Caco-2 cell are shown in Figure S3).
(B) To analyze whether TMPRSS2 can rescue SARS-2-S-driven entry into cells that have low CatB/L activity, 293T cells transiently expressing ACE2 alone or in combination with TMPRSS2 were incubated with CatB/L inhibitor E-64d or DMSO as control and inoculated with pseudotypes bearing the indicated viral surface proteins.
(C) Calu-3 cells were preincubated with the indicated concentrations of camostat mesylate and subsequently inoculated with pseudoparticles harboring the indicated viral glycoproteins.
(D) Calu-3 cells were preincubated with camostat mesylate and infected with SARS-CoV-2, washed and genome equivalents in culture supernatants determined by quantitative RT-PCR.
(E) In order to investigate whether serine protease activity is required for SARS-2-S-driven entry into human lung cells, primary human airway epithelial cells were incubated with camostat mesylate prior to transduction.
The average of three independent experiments conducted with triplicate or quadruplicate samples is shown in panels A-E. Error bars indicate SEM. Statistical significance was tested by two-way ANOVA with Dunnett posttest. Cells that did not receive inhibitor served as reference in panels A, C, D and E while cells transfected with empty vector and not treated with inhibitor served as reference in panel B.

Figure 5. Sera from convalescent SARS patients cross-neutralizes SARS-2-S-driven entry
Pseudotypes harboring the indicated viral surface proteins were incubated with different dilutions of sera from three convalescent SARS patients or sera from rabbits immunized with the S1-subunit of SARS-S and subsequently inoculated onto Vero cells in order to evaluate cross-neutralization potential. The average of three independent experiments performed with triplicate

samples is shown. Error bars indicate SEM. Statistical analysis was performed using Dunnetts posttest. Statistical significance was tested by two-way ANOVA with Dunnett posttest.

SUPPLEMENTAL INFORMATION

Figure S1. Representative experiment included in the average shown in Figure 1C

The indicated cells lines were inoculated with pseudoparticles harboring the indicated viral glycoprotein or harboring no glycoprotein (no protein) and luciferase activities in cell lysates were determined at 16 h posttransduction. The experiment was performed with quadruplicate samples, the average ± SD is shown.

Figure S2. Extended version of the phylogenetic tree presented in panel B of Figure 2

Figure S3. Protease requirement for SARS-2-S driven entry and absence of unwanted cytotoxicity of camostat mesylate, Related to Figure 4

Importance of endosomal low pH (A) and activity of CatB/L or TMPRSS2 (B) for host cell entry of SARS-CoV-2 was evaluated by adding inhibitors to target cells prior to transduction. Ammonium chloride (A) blocks endosomal acidification while E-64d and camostat mesylate (B) block the activity of CatB/L and TMPRSS2, respectively. Entry into cells not treated with inhibitor was set as 100 %.

(C) Absence of cytotoxic effects of camostat mesylate. Calu-3 cells were treated with camostat mesylate identically as for infection experiments and cell viability was measured using a commercially available assay (CellTiter-Glo, Promega).

STAR METHODS

KEY RESOURCES TABLE

REAGENT or RESOURCE	SOURCE	IDENTIFIER
Antibodies		
Monoclonal anti-HA antibody produced in mouse	Sigma-Aldrich	Cat.#: H3663 RRID: AB_262051
Monoclonal anti-β-actin antibody produced in mouse	Sigma-Aldrich	Cat.#: A5441 RRID: AB_476744
Monoclonal anti-VSV-M (23H12) antibody	KeraFast	Cat.#: EB0011 RRID:AB_2734773
Polyclonal anti-ACE2 antibody	R&D Systems	Cat.#: AF933 RRID: AB_355722
Polyclonal anti-DC-SIGN antibody	Santa Cruz	Cat.#: sc-11038 RRID:AB_639038
Monoclonal anti-mouse, peroxidase-coupled	Dianova	Cat.#: 115-035-003 RRID:AB_10015289
Anti-VSV-G antibody (I1, produced from CRL-2700 mouse hybridoma cells)	ATCC	Cat.# CRL-2700 RRID:CVCL_G654
Bacterial and Virus Strains		
VSV*ΔG-FLuc	(Berger Rentsch and Zimmer, 2011)	N/A
SARS-CoV-2 isolate Munich 929	Laboratory of Christian Drosten	N/A
One Shot™ OmniMAX™ 2 T1R Chemically Competent *E. coli*	ThermoFisher Scientific	Cat.#: C854003
Biological Samples		
Patient serum, CSS-2	Laboratory of Christian Drosten	N/A
Patient serum, CSS-3	Laboratory of Andreas Nitsche	N/A
Patient serum, CSS-4	Laboratory of Andreas Nitsche	N/A
Patient serum, CSS-5	Laboratory of Andreas Nitsche	N/A
Rabbit serum, anti-SARS-S1 rabbit I	Laboratory of Stefan Pöhlmann	N/A
Rabbit serum, anti-SARS-S1 rabbit II	Laboratory of Stefan Pöhlmann	N/A
Chemicals, Peptides, and Recombinant Proteins		
Camostat mesylate	Sigma-Aldrich	SML0057
E-64d	Sigma-Aldrich	E8640
Ammonium chloride	Carl Roth	Cat.#: 5050.2
Critical Commercial Assays		
Beetle-Juice Kit	PJK	Cat.#: 102511
CellTiter-Glo® Luminescent Cell Viability Assay	Promega	Cat.#: G7570
Deposited Data		
N/A	N/A	N/A
Experimental Models: Cell Lines		

A549	Laboratory of Georg Herrler	ATCC Cat# CRM-CCL-185 RRID:CVCL_0023
BEAS-2B	Laboratory of Stefan Pöhlmann	ATCC Cat# CRL-9609 RRID:CVCL_0168
Calu-3	Laboratory of Stephan Ludwig	ATCC Cat# HTB-55 RRID:CVCL_0609
NCI-H1299	Laboratory of Stefan Pöhlmann	ATCC Cat# CRL-5803 RRID:CVCL_0060
Huh-7	Laboratory of Thomas Pietschmann	JCRB Cat# JCRB0403 RRID:CVCL_0336
Caco-2	Laboratory of Stefan Pöhlmann	ATCC Cat# HTB-37 RRID:CVCL_0025
Vero	Laboratory of Andrea Maisner	ATCC Cat# CRL-1586 RRID:CVCL_0574
Vero-TMPRSS2	This paper	N/A
LLC-PK1	Laboratory of Georg Herrler	ATCC Cat# CRL-1392 RRID:CVCL_0391
MDBK	Laboratory of Georg Herrler	ATCC Cat# CCL-22 RRID:CVCL_0421
MDCKII	Laboratory of Georg Herrler	ATCC Cat# CRL-2936 RRID:CVCL_B034
RhiLu/1.1	Laboratory of Christian Drosten, Laboratory of Marcel A. Müller	N/A RRID: CVCL_RX22
MyDauLu/47.1	Laboratory of Christian Drosten, Laboratory of Marcel A. Müller	N/A RRID: CVCL_RX18
BHK-21	Laboratory of Georg Herrler	ATCC Cat# CCL-10 RRID:CVCL_1915
NIH/3T3	Laboratory of Stefan Pöhlmann	ATCC Cat# CRL-1658 RRID:CVCL_0594
HAE	HTCR Foundation (Human Tissue and Cell Research)	N/A
293T	DSMZ	Cat.#: ACC-635 RRID: CVCL_0063
Experimental Models: Organisms/Strains		
N/A	N/A	N/A
Oligonucleotides		
SARS-2-S (BamHI) F AAGGCCGGATCCGCCACCATGTTTCTGCTGACCACCAAGC	Sigma-Aldrich	N/A
SARS-2-S (XbaI) R AAGGCCTCTAGATTAGGTGTAGTGCAGTTTCACG	Sigma-Aldrich	N/A
SARS-2-S-HA (XbaI) R AAGGCCTCTAGATTACGCATAATCCGGCACATCATACGGATAGGTGTAGTGCAGTTTCACG	Sigma-Aldrich	N/A

WH-Ssyn 651F CAAGATCTACAGCAAGCACACC	Sigma-Aldrich	N/A
WH-Ssyn 1380F GTCGGCGGCAACTACAATTAC	Sigma-Aldrich	N/A
WH-Ssyn 1992F CTGTCTGATCGGAGCCGAGCAC	Sigma-Aldrich	N/A
WH-Ssyn 2648F TGAGATGATCGCCCAGTACAC	Sigma-Aldrich	N/A
WH-Ssyn 3286F GCCATCTGCCACGACGGCAAAG	Sigma-Aldrich	N/A
Recombinant DNA		
Synthetic, codon-optimized (humanized) SARS-2-S	ThermoFisher Scientific (GeneArt)	N/A
Plasmid: pCG1-SARS-S	(Hoffmann et al., 2013)	N/A
Plasmid:pCG1-SARS-S-HA	This paper	N/A
Plasmid: pCG1-SARS-2-S	This paper	N/A
Plasmid: pCG1-SARS-2-S-HA	This paper	N/A
Plasmid: pCAGGS-229E-S	(Hofmann et al., 2005)	N/A
Plasmid: pCAGGS-MERS-S	(Gierer et al., 2013)	N/A
Plasmid: pCAGGS-VSV-G	(Brinkmann et al., 2017)	N/A
Plasmid: pCAGGS-NiV-F	Laboratory of Andrea Maisner	N/A
Plasmid: pCAGGS-NiV-G	Laboratory of Andrea Maisner	N/A
Plasmid: pCG1-hACE2	(Hoffmann et al., 2013)	N/A
Plasmid: pCG1-batACE2	(Hoffmann et al., 2013)	N/A
Plasmid: pCG1-hAPN	(Hofmann et al., 2004a)	N/A
Plasmid: pQCXIP-DsRed-hDPP4	(Kleine-Weber et al., 2018)	N/A
Plasmid: pQCXIBL-hTMPRSS2	(Kleine-Weber et al., 2018)	N/A
Plasmid: pCG1	Laboratory of Roberto Cattaneo	N/A
Plasmid: pCAGGS-DsRed	Laboratory of Stefan Pöhlmann	N/A
Plasmid: pCAGGS-eGFP	Laboratory of Stefan Pöhlmann	N/A
Software and Algorithms		
Hidex Sense Microplate Reader Software	Hidex Deutschland Vertrieb GmbH	https://www.hidex.de/
ChemoStar Imager Software (version v.0.3.23)	Intas Science Imaging Instruments GmbH	https://www.intas.de/
MEGA 7.0.26	Kumar et al., 2018	https://www.megasoftware.net
Adobe Photoshop CS5 Extended (version 12.0 x 32)	Adobe	https://www.adobe.com/
GraphPad Prism (version 8.3.0(538))	GraphPad Software	https://www.graphpad.com/
Microsoft Office Standard 2010 (version 14.0.7232.5000)	Microsoft Corporation	https://products.office.com/
Other		
N/A	N/A	N/A

LEAD CONTACT AND MATERIALS AVAILABILITY

Requests for material can be directed to Markus Hoffmann (mhoffmann@dpz.eu) and the lead contact, Stefan Pöhlmann (spoehlmann@dpz.eu). All materials and reagents will be made available upon installment of a material transfer agreement (MTA).

EXPERIMANTAL MODEL AND SUBJECT DETAILS

Cell cultures, primary cells, viral strains

All cell lines were incubated at 37 °C and 5 % CO_2 in a humidified atmosphere. 293T (human, kidney), BHK-21 (Syrian hamster, kidney cells), Huh-7 (human, liver), LLC-PK1 (pig, kidney), MRC-5 (human, lung), MyDauLu/47.1 (Daubenton's bat [*Myotis daubentonii*], lung), NIH/3T3 (Mouse, embryo), RhiLu/1.1 (Halcyon horseshoe bat [*Rhinolophus alcyone*], lung) and Vero (African green monkey, kidney) cells were incubated in Dulbecco's' modified Eagle medium (PAN-Biotech). Calu-3 (human, lung), Caco-2 (human, colon), MDBK (cattle, kidney) and MDCKII (Dog, kidney) cells were incubated in Minimum Essential Medium (ThermoFisher Scientific). A549 (human, lung), BEAS-2B (human, bronchus) and NCI-H1299 (human, lung) cells were incubated in DMEM/F-12 Medium with Nutrient Mix (ThermoFisher Scientific). Vero cells stably expressing human TMPRSS2 were generated by retroviral transduction and blasticidin-based selection. All media were supplemented with 10 % fetal bovine serum (Biochrom), 100 U/ml of penicillin and 0.1 mg/ml of streptomycin (PAN-Biotech), 1x non-essential amino acid solution (10x stock, PAA) and 10 mM sodium pyruvate (ThermoFisher Scientific). For seeding and subcultivation, cells were first washed with phosphate buffered saline (PBS) and then incubated in the presence of trypsin/EDTA solution (PAN-Biotech) until cells detached. Transfection was carried out by calcium-phosphate precipitation. Lung tissue samples

were obtained and experimental procedures were performed within the framework of the non-profit foundation HTCR, including the informed patient's consent.

For preparation of human airway epithelial cells, bronchus tissue was derived from patients undergoing pulmonary resection and was provided by the Biobank of the Department of General, Visceral, and Transplant Surgery, Ludwig-Maximilians- University Munich. Primary human airway epithelial cells were subsequently isolated as described (Wu et al., 2016). In brief, tissue with a length of approximately 10 mm and a diameter of 8mm was collected and incubated for 24 h at 4°C with DMEM (GIBCO) containing 1 mg/ml protease type XIV and 10 µg/ml DNase I, 100 units/ml penicillin and 100 µg/ml streptomycin, 2.5 µg/ml amphotericin B, and 50 µg/ml gentamicin (GIBCO). The epithelial cells were then harvested from the mucosal surface using the scalpel and were resuspended in growth medium. After incubation at 37°C, 5% CO_2 for 2 h to remove adherent fibroblast cells, non-adherent cells were seeded on a collagen I coated flask and maintained at 37°C, 5% CO_2. The growth medium was refreshed every 2 days and consisted of a 1:1 mixture of DMEM (GIBCO) and Airway Epithelial Cell basal medium (Promocell, Heidelberg, Germany) supplemented with 52 µg/ml bovine pituitary extract, 15 ng/ml retinoic acid, 5µg/ml insulin, 0.5 µg/ml hydrocortisone, 0.5 µg/ml epinephrine, 10 µg/ml transferrin, 1 ng/ml human epidermal growth factor (Corning), 1.5 ng/ml bovine serum albumin, 100 µg/ml penicillin and 100 µg/ml streptomycin, with or without 5 µM Rho-associated protein kinase inhibitor (Y-27632), as previously described (Wu et al., 2016). If not stated otherwise all materials were purchased from Sigma-Aldrich.

For infection experiments with SARS-CoV-2, the SARS-CoV-2 isolate Munich 929 was propagated in VeroE6 cells (passage 1) after primary isolation from patient material on Vero-TMPRSS2 cells (passage 0).

METHOD DETAILS

Plasmids

Expression plasmids for vesicular stomatitis virus (VSV, serotype Indiana) glycoprotein (VSV-G), Nipah virus (NiV) fusion (F) and attachment glycoprotein (G), SARS-S (derived from the Frankfurt-1 isolate) with or without a C-terminal HA epitope tag, HCoV-229E-S, MERS-S, human and bat angiotensin converting enzyme 2 (ACE2), human aminopeptidase N (APN), human dipeptidyl-peptidase 4 (DPP4) and human TMPRSS2 have been described elsewhere (Bertram et al., 2010; Brinkmann et al., 2017; Gierer et al., 2013; Hoffmann et al., 2013; Hofmann et al., 2005; Kleine-Weber et al., 2019). For generation of the expression plasmids for SARS-2-S with or without a C-terminal HA epitope tag we PCR-amplified the coding sequence of a synthetic, codon-optimized (for human cells) SARS-2-S DNA (GeneArt Gene Synthesis, ThermoFisher Scientific) based on the publicly available protein sequence in the National Center for Biotechnology Information database (NCBI Reference Sequence: YP_009724390.1) and cloned in into the pCG1 expression vector via BamHI and XbaI restriction sites.

Pseudotyping of VSV and transduction experiments

For pseudotyping, VSV pseudotypes were generated according to a published protocol (Berger Rentsch and Zimmer, 2011). In brief, 293T transfected to express the viral surface glycoprotein under study were inoculated with a replication-deficient VSV vector that contains expression cassettes for eGFP (enhanced green fluorescent protein) and firefly luciferase instead of the VSV-G open reading frame, VSV*ΔG-fLuc (kindly provided by Gert Zimmer, Institute of Virology and Immunology, Mittelhäusern/Switzerland). After an incubation period of 1 h at 37 °C, the inoculum was removed and cells were washed with PBS before medium supplemented with anti-

VSV-G antibody (I1, mouse hybridoma supernatant from CRL-2700; ATCC) was added in order to neutralize residual input virus (no antibody was added to cells expressing VSV-G). Pseudotyped particles were harvested 16 h postinoculation, clarified from cellular debris by centrifugation and used for experimentation.

For transduction, target cells were grown in 96-well plates until they reached 50-75 % confluency before they were inoculated with respective pseudotyped VSV. For experiments addressing receptor usage, cells were transfected with expression plasmids 24 h before transduction. In order to block ACE2 on the cell surface, cells were pretreated with 2 or 20 µg/ml anti-ACE2 antibody (R&D Systems, goat, AF933). As control, an unrelated anti-DC-SIGN antibody (Serotec, goat, 20 µg/ml) was used. For experiments involving ammonium chloride (final concentration 50 mM) and protease inhibitors (E-64d, 25 µM; camostat mesylate, 1-500 µM), target cells were treated with the respective chemical 2 h before transduction. For neutralization experiments, pseudotypes were pre-incubated for 30 min at 37 °C with different serum dilutions. Transduction efficiency was quantified 16 h posttransduction by measuring the activity of firefly luciferase in cell lysates using a commercial substrate (Beetle-Juice, PJK) and a Hidex Sense plate luminometer (Hidex).

Quantification of cell viability

Cell viability following treatment of Calu-3 cells with camostat mesylate was analyzed using the CellTiter-Glo® Luminescent Cell Viability Assay (Promega). In brief, Calu-3 cells grown to 50 % confluency in 96-well plates were incubated for 24 h in the absence or presence of different concentrations (1-500 µM) of camostat mesylate. Next, the culture medium was aspirated and 100 µl of fresh culture medium was added before an identical volume of the assay substrate was added. Wells containing only culture medium served as a control to determine the assay

555 background. After 2 min of incubation on a rocking platform and additional 10 min without
556 movement, samples were transferred into white opaque-walled 96-well plates and luminescent
557 signal were recorded using a Hidex Sense plate luminometer (Hidex).
558
559 **Analysis of SARS-2-S expression and particle incorporation**
560 To analyze S protein expression in cells, 293T cells were transfected with expression vectors for
561 HA-tagged SARS-2-S or SARS-S or empty expression vector (negative control). The culture
562 medium was replaced at 16 h posttransfection and the cells were incubated for an additional 24 h.
563 Then, the culture medium was removed and cells were washed once with PBS before 2x SDS-
564 sample buffer (0.03 M Tris-HCl, 10% glycerol, 2% SDS, 0.2% bromophenol blue, 1 mM EDTA)
565 was added and cells were incubated for 10 min at room temperature. Next, the samples were
566 heated for 15 min at 96 °C and subjected to SDS-PAGE and immunoblotting.
567 For analysis of S protein incorporation into pseudotyped particles, 1 ml of the respective
568 VSV pseudotypes were loaded onto a 20 % (w/v) sucrose cushion (volume 50 µl) and subjected
569 to high-speed centrifugation (25.000 g for 120 min at 4 °C). Thereafter, 1 ml of supernatant was
570 removed and the residual volume was mixed with 50 µl of 2x SDS-sample buffer, heated for 15
571 min at 96 °C and subjected to SDS-PAGE and immunoblotting. After protein transfer,
572 nitrocellulose membranes were blocked in 5 % skim milk solution (5 % skim milk dissolved in
573 PBS containing 0.05 % Tween-20, PBS-T) for 1 h at room temperature and then incubated over
574 night at 4 °C with the primary antibody (diluted in in skim milk solution)). Following three
575 washing intervals of 10 min in PBS-T the membranes were incubated for 1 h at room temperature
576 with the secondary antibody (diluted in in skim milk solution), before the membranes were
577 washed and imaged using an in in house-prepared enhanced chemiluminescent solution (0.1 M
578 Tris-HCl [pH 8.6], 250 µg/ml luminol, 1 mg/ml para-hydroxycoumaric acid, 0.3 % H_2O^2) and the

ChemoCam imaging system along with the ChemoStar Professional software (Intas Science Imaging Instruments GmbH). The following primary antibodies were used: Mouse anti-HA tag (Sigma-Aldrich, H3663, 1:2,500), mouse anti-ß-actin (Sigma-Aldrich, A5441, 1:2,000), mouse anti-VSV matrix protein (Kerafast, EB0011, 1:2,500). As secondary antibody we used a peroxidase-coupled goat anti-mouse antibody (Dianova, 115-035-003, 1:10000).

Infection with authentic SARS-CoV-2

BHK-21 cells (1.6 x10^5 cells/ml) were transfected with ACE2 and DsRed as a negative control. After 24 h, cells were washed with PBS and infected with 8x10^7 genome equivalents (GE) per 24-well of SARS-CoV-2 isolate Munich 929 for 1 hour at 37°C. Calu-3 cells (5 x10^5 cells/ml) were mock treated or treated with 100 µM camostat mesylate (Sigma Aldrich) 2 h prior to infection with SARS-CoV-2 isolate Munich 929 at a multiplicity of infection (MOI) of 0.001 for 1 h at 37°C. After infection, cells were washed three times with PBS before 500 µl of DMEM medium was added. At 16 or 24 h post infection, 50 µl culture supernatant was subjected to viral RNA extraction using a viral RNA kit (Macherey-Nagel) according to the manufacturer's instructions. GE per ml were detected by real time RT-PCR using a previously reported protocol (Corman et al., 2020).

Sera

The convalescent human anti-SARS-CoV sera (CSS-2 to CSS-5) stemmed from the serum collection of the national consiliary laboratory for coronavirus diagnostics at Charité, Berlin, Germany or the Robert Koch Institute, Berlin, Germany. All sera were previously tested positive using a recombinant S-based immunofluorescence test (Buchholz et al., 2013). CSS-2 was taken from a SARS patient 3.5 years post onset of disease. CSS-3 and CSS-4 originated from a second

SARS patient 24 and 36 days post onset of disease. CSS-5 was collected from a third SARS patient 10 days post onset of disease. Rabbit sera were obtained by immunizing rabbits with purified SARS-S1 protein fused to the Fc portion of human immunoglobulin.

Phylogenetic analysis

Phylogenetic analysis (neighbor-joining tree, bootstrap method with 5,000 iterations, Poisson substitution model, uniform rates among sites, complete deletion of gaps/missing data) was performed using the MEGA7.0.26 software. Reference sequences were obtained from the National Center for Biotechnology Information and GISAID (Global Initiative on Sharing All Influenza Data) databases. Reference numbers are indicated in the figures.

QUANTIFICATION AND STATISTICAL ANALYSIS

One-way or two-way analysis of variance (ANOVA) with Dunnett posttest was used to test for statistical significance. Only p values of 0.05 or lower were considered statistically significant ($p > 0.05$ [ns, not significant], $p \leq 0.05$ [*], $p \leq 0.01$ [**], $p \leq 0.001$ [***]). For all statistical analyses, the GraphPad Prism 7 software package was used (GraphPad Software).

DATA AND CODE AVAILABILITY

The study did not generate unique datasets or code.

REFERENCES

Berger Rentsch, M., and Zimmer, G. (2011). A vesicular stomatitis virus replicon-based bioassay for the rapid and sensitive determination of multi-species type I interferon. PLoS One *6*, e25858.

Bertram, S., Glowacka, I., Blazejewska, P., Soilleux, E., Allen, P., Danisch, S., Steffen, I., Choi, S.Y., Park, Y., Schneider, H., *et al.* (2010). TMPRSS2 and TMPRSS4 facilitate trypsin-independent spread of influenza virus in Caco-2 cells. J Virol *84*, 10016-10025.

Bertram, S., Heurich, A., Lavender, H., Gierer, S., Danisch, S., Perin, P., Lucas, J.M., Nelson, P.S., Pöhlmann, S., and Soilleux, E.J. (2012). Influenza and SARS-coronavirus activating proteases TMPRSS2 and HAT are expressed at multiple sites in human respiratory and gastrointestinal tracts. PLoS One *7*, e35876.

Bossart, K.N., Wang, L.F., Flora, M.N., Chua, K.B., Lam, S.K., Eaton, B.T., and Broder, C.C. (2002). Membrane fusion tropism and heterotypic functional activities of the Nipah virus and Hendra virus envelope glycoproteins. J Virol *76*, 11186-11198.

Brinkmann, C., Hoffmann, M., Lubke, A., Nehlmeier, I., Kramer-Kuhl, A., Winkler, M., and Pöhlmann, S. (2017). The glycoprotein of vesicular stomatitis virus promotes release of virus-like particles from tetherin-positive cells. PLoS One *12*, e0189073.

Buchholz, U., Muller, M.A., Nitsche, A., Sanewski, A., Wevering, N., Bauer-Balci, T., Bonin, F., Drosten, C., Schweiger, B., Wolff, T., *et al.* (2013). Contact investigation of a case of human novel coronavirus infection treated in a German hospital, October-November 2012. Euro Surveill *18*.

Chan, J.F., Yuan, S., Kok, K.H., To, K.K., Chu, H., Yang, J., Xing, F., Liu, J., Yip, C.C., Poon, R.W., *et al.* (2020). A familial cluster of pneumonia associated with the 2019 novel coronavirus indicating person-to-person transmission: a study of a family cluster. Lancet.

Corman, V.M., Landt, O., Kaiser, M., Molenkamp, R., Meijer, A., Chu, D.K., Bleicker, T., Brunink, S., Schneider, J., Schmidt, M.L., *et al.* (2020). Detection of 2019 novel coronavirus (2019-nCoV) by real-time RT-PCR. Euro Surveill *25*.

Corman, V.M., Lienau, J., and Witzenrath, M. (2019). [Coronaviruses as the cause of respiratory infections]. Internist (Berl) *60*, 1136-1145.

de Wit, E., van Doremalen, N., Falzarano, D., and Munster, V.J. (2016). SARS and MERS: recent insights into emerging coronaviruses. Nat Rev Microbiol *14*, 523-534.

Ding, Y., He, L., Zhang, Q., Huang, Z., Che, X., Hou, J., Wang, H., Shen, H., Qiu, L., Li, Z., *et al.* (2004). Organ distribution of severe acute respiratory syndrome (SARS) associated coronavirus (SARS-CoV) in SARS patients: implications for pathogenesis and virus transmission pathways. J Pathol *203*, 622-630.

Fehr, A.R., Channappanavar, R., and Perlman, S. (2017). Middle East Respiratory Syndrome: Emergence of a Pathogenic Human Coronavirus. Annu Rev Med *68*, 387-399.

Ge, X.Y., Li, J.L., Yang, X.L., Chmura, A.A., Zhu, G., Epstein, J.H., Mazet, J.K., Hu, B., Zhang, W., Peng, C., *et al.* (2013). Isolation and characterization of a bat SARS-like coronavirus that uses the ACE2 receptor. Nature *503*, 535-538.

Gierer, S., Bertram, S., Kaup, F., Wrensch, F., Heurich, A., Kramer-Kuhl, A., Welsch, K., Winkler, M., Meyer, B., Drosten, C., *et al.* (2013). The spike protein of the emerging

668 betacoronavirus EMC uses a novel coronavirus receptor for entry, can be activated by TMPRSS2,
669 and is targeted by neutralizing antibodies. J Virol *87*, 5502-5511.

670 Glowacka, I., Bertram, S., Muller, M.A., Allen, P., Soilleux, E., Pfefferle, S., Steffen, I., Tsegaye,
671 T.S., He, Y., Gnirss, K., *et al.* (2011). Evidence that TMPRSS2 activates the severe acute
672 respiratory syndrome coronavirus spike protein for membrane fusion and reduces viral control by
673 the humoral immune response. J Virol *85*, 4122-4134.

674 Gu, J., Gong, E., Zhang, B., Zheng, J., Gao, Z., Zhong, Y., Zou, W., Zhan, J., Wang, S., Xie, Z.,
675 *et al.* (2005). Multiple organ infection and the pathogenesis of SARS. J Exp Med *202*, 415-424.

676 Guan, Y., Zheng, B.J., He, Y.Q., Liu, X.L., Zhuang, Z.X., Cheung, C.L., Luo, S.W., Li, P.H.,
677 Zhang, L.J., Guan, Y.J., *et al.* (2003). Isolation and characterization of viruses related to the
678 SARS coronavirus from animals in southern China. Science *302*, 276-278.

679 Haga, S., Yamamoto, N., Nakai-Murakami, C., Osawa, Y., Tokunaga, K., Sata, T., Yamamoto,
680 N., Sasazuki, T., and Ishizaka, Y. (2008). Modulation of TNF-alpha-converting enzyme by the
681 spike protein of SARS-CoV and ACE2 induces TNF-alpha production and facilitates viral entry.
682 Proc Natl Acad Sci U S A *105*, 7809-7814.

683 Hamming, I., Timens, W., Bulthuis, M.L., Lely, A.T., Navis, G., and van Goor, H. (2004). Tissue
684 distribution of ACE2 protein, the functional receptor for SARS coronavirus. A first step in
685 understanding SARS pathogenesis. J Pathol *203*, 631-637.

686 He, Y., Li, J., Heck, S., Lustigman, S., and Jiang, S. (2006). Antigenic and immunogenic
687 characterization of recombinant baculovirus-expressed severe acute respiratory syndrome
688 coronavirus spike protein: implication for vaccine design. J Virol *80*, 5757-5767.

689 Hoffmann, M., Muller, M.A., Drexler, J.F., Glende, J., Erdt, M., Gutzkow, T., Losemann, C.,
690 Binger, T., Deng, H., Schwegmann-Wessels, C., *et al.* (2013). Differential sensitivity of bat cells
691 to infection by enveloped RNA viruses: coronaviruses, paramyxoviruses, filoviruses, and
692 influenza viruses. PLoS One *8*, e72942.

693 Hofmann, H., Geier, M., Marzi, A., Krumbiegel, M., Peipp, M., Fey, G.H., Gramberg, T., and
694 Pöhlmann, S. (2004a). Susceptibility to SARS coronavirus S protein-driven infection correlates
695 with expression of angiotensin converting enzyme 2 and infection can be blocked by soluble
696 receptor. Biochem Biophys Res Commun *319*, 1216-1221.

697 Hofmann, H., Hattermann, K., Marzi, A., Gramberg, T., Geier, M., Krumbiegel, M., Kuate, S.,
698 Uberla, K., Niedrig, M., and Pöhlmann, S. (2004b). S protein of severe acute respiratory
699 syndrome-associated coronavirus mediates entry into hepatoma cell lines and is targeted by
700 neutralizing antibodies in infected patients. J Virol *78*, 6134-6142.

701 Hofmann, H., Pyrc, K., van der Hoek, L., Geier, M., Berkhout, B., and Pöhlmann, S. (2005).
702 Human coronavirus NL63 employs the severe acute respiratory syndrome coronavirus receptor
703 for cellular entry. Proc Natl Acad Sci U S A *102*, 7988-7993.

704 Huang, C., Wang, Y., Li, X., Ren, L., Zhao, J., Hu, Y., Zhang, L., Fan, G., Xu, J., Gu, X., *et al.*
705 (2020). Clinical features of patients infected with 2019 novel coronavirus in Wuhan, China.
706 Lancet.

707 Imai, Y., Kuba, K., Rao, S., Huan, Y., Guo, F., Guan, B., Yang, P., Sarao, R., Wada, T., Leong-
708 Poi, H., *et al.* (2005). Angiotensin-converting enzyme 2 protects from severe acute lung failure.
709 Nature *436*, 112-116.

Iwata-Yoshikawa, N., Okamura, T., Shimizu, Y., Hasegawa, H., Takeda, M., and Nagata, N. (2019). TMPRSS2 Contributes to Virus Spread and Immunopathology in the Airways of Murine Models after Coronavirus Infection. J Virol *93*.

Kawase, M., Shirato, K., van der Hoek, L., Taguchi, F., and Matsuyama, S. (2012). Simultaneous treatment of human bronchial epithelial cells with serine and cysteine protease inhibitors prevents severe acute respiratory syndrome coronavirus entry. J Virol *86*, 6537-6545.

Kim, T.S., Heinlein, C., Hackman, R.C., and Nelson, P.S. (2006). Phenotypic analysis of mice lacking the Tmprss2-encoded protease. Mol Cell Biol *26*, 965-975.

Kleine-Weber, H., Elzayat, M.T., Hoffmann, M., and Pöhlmann, S. (2018). Functional analysis of potential cleavage sites in the MERS-coronavirus spike protein. Sci Rep *8*, 16597.

Kleine-Weber, H., Elzayat, M.T., Wang, L., Graham, B.S., Muller, M.A., Drosten, C., Pöhlmann, S., and Hoffmann, M. (2019). Mutations in the Spike Protein of Middle East Respiratory Syndrome Coronavirus Transmitted in Korea Increase Resistance to Antibody-Mediated Neutralization. J Virol *93*.

Kuba, K., Imai, Y., Rao, S., Gao, H., Guo, F., Guan, B., Huan, Y., Yang, P., Zhang, Y., Deng, W., *et al.* (2005). A crucial role of angiotensin converting enzyme 2 (ACE2) in SARS coronavirus-induced lung injury. Nat Med *11*, 875-879.

Lau, S.K., Woo, P.C., Li, K.S., Huang, Y., Tsoi, H.W., Wong, B.H., Wong, S.S., Leung, S.Y., Chan, K.H., and Yuen, K.Y. (2005). Severe acute respiratory syndrome coronavirus-like virus in Chinese horseshoe bats. Proc Natl Acad Sci U S A *102*, 14040-14045.

730 Li, F., Li, W., Farzan, M., and Harrison, S.C. (2005a). Structure of SARS coronavirus spike
731 receptor-binding domain complexed with receptor. Science *309*, 1864-1868.

732 Li, W., Hulswit, R.J.G., Widjaja, I., Raj, V.S., McBride, R., Peng, W., Widagdo, W., Tortorici,
733 M.A., van Dieren, B., Lang, Y., *et al.* (2017). Identification of sialic acid-binding function for the
734 Middle East respiratory syndrome coronavirus spike glycoprotein. Proc Natl Acad Sci U S A
735 *114*, E8508-E8517.

736 Li, W., Moore, M.J., Vasilieva, N., Sui, J., Wong, S.K., Berne, M.A., Somasundaran, M.,
737 Sullivan, J.L., Luzuriaga, K., Greenough, T.C., *et al.* (2003). Angiotensin-converting enzyme 2 is
738 a functional receptor for the SARS coronavirus. Nature *426*, 450-454.

739 Li, W., Zhang, C., Sui, J., Kuhn, J.H., Moore, M.J., Luo, S., Wong, S.K., Huang, I.C., Xu, K.,
740 Vasilieva, N., *et al.* (2005b). Receptor and viral determinants of SARS-coronavirus adaptation to
741 human ACE2. EMBO J *24*, 1634-1643.

742 Lin, J.T., Zhang, J.S., Su, N., Xu, J.G., Wang, N., Chen, J.T., Chen, X., Liu, Y.X., Gao, H., Jia,
743 Y.P., *et al.* (2007). Safety and immunogenicity from a phase I trial of inactivated severe acute
744 respiratory syndrome coronavirus vaccine. Antivir Ther *12*, 1107-1113.

745 Liu, W., Fontanet, A., Zhang, P.H., Zhan, L., Xin, Z.T., Baril, L., Tang, F., Lv, H., and Cao,
746 W.C. (2006). Two-year prospective study of the humoral immune response of patients with
747 severe acute respiratory syndrome. J Infect Dis *193*, 792-795.

748 Matsuyama, S., Nagata, N., Shirato, K., Kawase, M., Takeda, M., and Taguchi, F. (2010).
749 Efficient activation of the severe acute respiratory syndrome coronavirus spike protein by the
750 transmembrane protease TMPRSS2. J Virol *84*, 12658-12664.

751 Menachery, V.D., Dinnon, K.H., 3rd, Yount, B.L., Jr., McAnarney, E.T., Gralinski, L.E., Hale,
752 A., Graham, R.L., Scobey, T., Anthony, S.J., Wang, L., *et al.* (2019). Trypsin treatment unlocks
753 barrier for zoonotic bat coronaviruses infection. J Virol.

754 Munster, V.J., Koopmans, M., van Doremalen, N., van Riel, D., and de Wit, E. (2020). A Novel
755 Coronavirus Emerging in China - Key Questions for Impact Assessment. N Engl J Med.

756 Park, J.E., Li, K., Barlan, A., Fehr, A.R., Perlman, S., McCray, P.B., Jr., and Gallagher, T.
757 (2016). Proteolytic processing of Middle East respiratory syndrome coronavirus spikes expands
758 virus tropism. Proc Natl Acad Sci U S A *113*, 12262-12267.

759 Park, Y.J., Walls, A.C., Wang, Z., Sauer, M.M., Li, W., Tortorici, M.A., Bosch, B.J., DiMaio, F.,
760 and Veesler, D. (2019). Structures of MERS-CoV spike glycoprotein in complex with sialoside
761 attachment receptors. Nat Struct Mol Biol *26*, 1151-1157.

762 Raj, V.S., Mou, H., Smits, S.L., Dekkers, D.H., Muller, M.A., Dijkman, R., Muth, D., Demmers,
763 J.A., Zaki, A., Fouchier, R.A., *et al.* (2013). Dipeptidyl peptidase 4 is a functional receptor for the
764 emerging human coronavirus-EMC. Nature *495*, 251-254.

765 Shieh, W.J., Hsiao, C.H., Paddock, C.D., Guarner, J., Goldsmith, C.S., Tatti, K., Packard, M.,
766 Mueller, L., Wu, M.Z., Rollin, P., *et al.* (2005). Immunohistochemical, in situ hybridization, and
767 ultrastructural localization of SARS-associated coronavirus in lung of a fatal case of severe acute
768 respiratory syndrome in Taiwan. Hum Pathol *36*, 303-309.

769 Shirato, K., Kanou, K., Kawase, M., and Matsuyama, S. (2017). Clinical Isolates of Human
770 Coronavirus 229E Bypass the Endosome for Cell Entry. J Virol *91*.

771 Shirato, K., Kawase, M., and Matsuyama, S. (2018). Wild-type human coronaviruses prefer cell-
772 surface TMPRSS2 to endosomal cathepsins for cell entry. Virology *517*, 9-15.

773 Shulla, A., Heald-Sargent, T., Subramanya, G., Zhao, J., Perlman, S., and Gallagher, T. (2011). A
774 transmembrane serine protease is linked to the severe acute respiratory syndrome coronavirus
775 receptor and activates virus entry. J Virol *85*, 873-882.

776 Simmons, G., Gosalia, D.N., Rennekamp, A.J., Reeves, J.D., Diamond, S.L., and Bates, P.
777 (2005). Inhibitors of cathepsin L prevent severe acute respiratory syndrome coronavirus entry.
778 Proc Natl Acad Sci U S A *102*, 11876-11881.

779 Wang, C., Horby, P.W., Hayden, F.G., and Gao, G.F. (2020). A novel coronavirus outbreak of
780 global health concern. Lancet.

781 WHO (2004). Summary of probable SARS cases with onset of illness from 1 November 2002 to
782 31 July 2003

783 WHO (2020). Novel Coronavirus(2019-nCoV) Situation Report 23.

784 Wu, N.H., Yang, W., Beineke, A., Dijkman, R., Matrosovich, M., Baumgartner, W., Thiel, V.,
785 Valentin-Weigand, P., Meng, F., and Herrler, G. (2016). The differentiated airway epithelium
786 infected by influenza viruses maintains the barrier function despite a dramatic loss of ciliated
787 cells. Sci Rep *6*, 39668.

788 Yamamoto, M., Matsuyama, S., Li, X., Takeda, M., Kawaguchi, Y., Inoue, J.I., and Matsuda, Z.
789 (2016). Identification of Nafamostat as a Potent Inhibitor of Middle East Respiratory Syndrome
790 Coronavirus S Protein-Mediated Membrane Fusion Using the Split-Protein-Based Cell-Cell
791 Fusion Assay. Antimicrob Agents Chemother *60*, 6532-6539.

792 Yang, Y., Du, L., Liu, C., Wang, L., Ma, C., Tang, J., Baric, R.S., Jiang, S., and Li, F. (2014).
793 Receptor usage and cell entry of bat coronavirus HKU4 provide insight into bat-to-human
794 transmission of MERS coronavirus. Proc Natl Acad Sci U S A *111*, 12516-12521.

795 Yang, Y., Liu, C., Du, L., Jiang, S., Shi, Z., Baric, R.S., and Li, F. (2015). Two Mutations Were
796 Critical for Bat-to-Human Transmission of Middle East Respiratory Syndrome Coronavirus. J
797 Virol *89*, 9119-9123.

798 Yeager, C.L., Ashmun, R.A., Williams, R.K., Cardellichio, C.B., Shapiro, L.H., Look, A.T., and
799 Holmes, K.V. (1992). Human aminopeptidase N is a receptor for human coronavirus 229E.
800 Nature *357*, 420-422.

801 Zhou, P., Yang, X.L., Wang, X.G., Hu, B., Zhang, L., Zhang, W., Si, H.R., Zhu, Y., Li, B.,
802 Huang, C.L., *et al.* (2020). A pneumonia outbreak associated with a new coronavirus of probable
803 bat origin. Nature.

804 Zhou, Y., Vedantham, P., Lu, K., Agudelo, J., Carrion, R., Jr., Nunneley, J.W., Barnard, D.,
805 Pöhlmann, S., McKerrow, J.H., Renslo, A.R., *et al.* (2015). Protease inhibitors targeting
806 coronavirus and filovirus entry. Antiviral Res *116*, 76-84.

807 Zhu, N., Zhang, D., Wang, W., Li, X., Yang, B., Song, J., Zhao, X., Huang, B., Shi, W., Lu, R.,
808 *et al.* (2020). A Novel Coronavirus from Patients with Pneumonia in China, 2019. N Engl J Med.

809

810

811

812

Figure 1

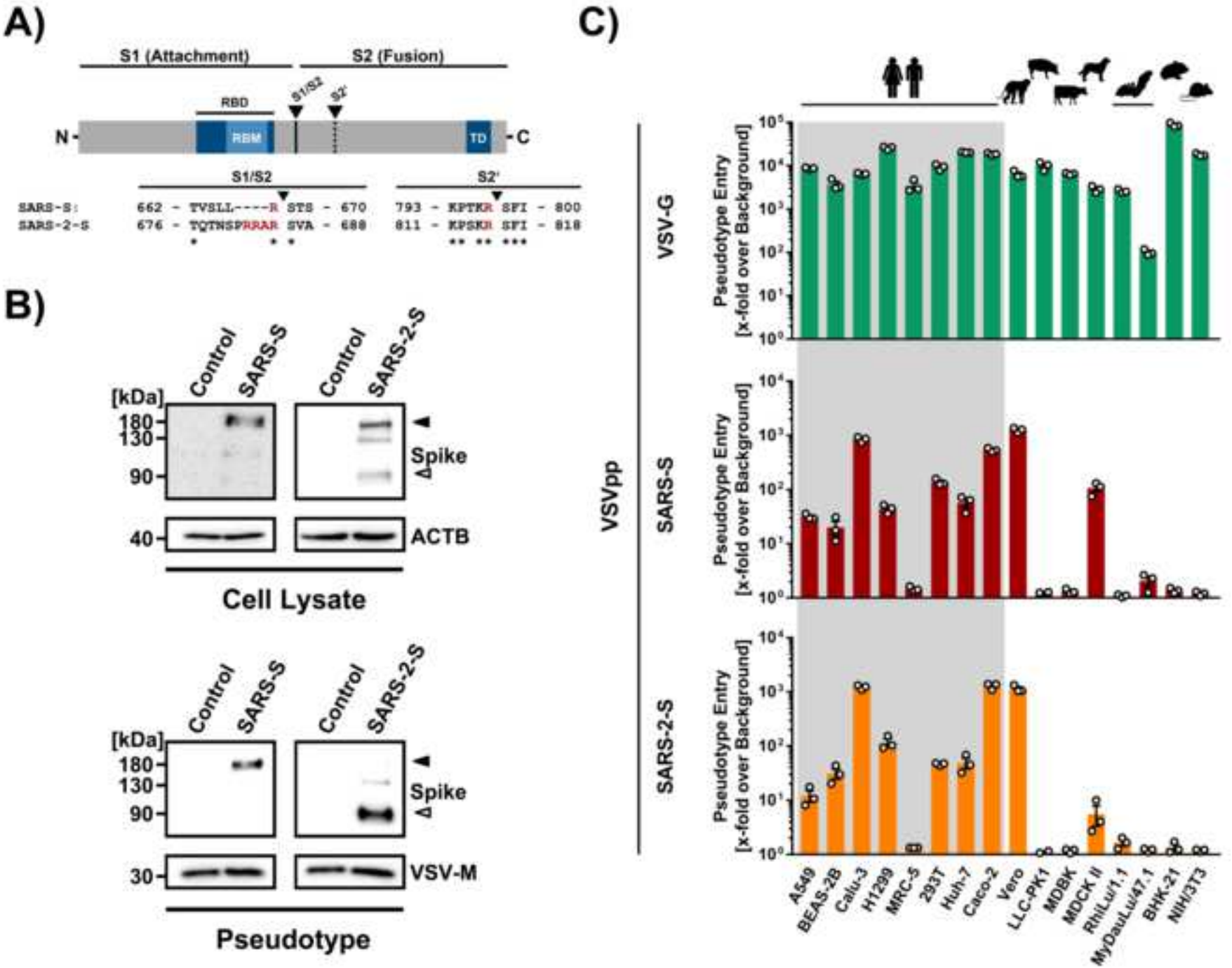
A)
S1 (Attachment)
S2 (Fusion)
RBD
S1/S2
S2'
N
RBM
TD
C
S1/S2
S2'
SARS-S: 662 - TVSLL----R STS - 670
SARS-2-S 676 - TQTNSPRRAR SVA - 688
793 - KPTKR SFI - 800
811 - KPSKR SFI - 818
B)
Control
SARS-S
Control
SARS-2-S
[kDa]
180
130
90
40
Spike
ACTB
Cell Lysate
Control
SARS-S
Control
SARS-2-S
[kDa]
180
130
90
30
Spike
VSV-M
Pseudotype
C)
VSVpp
VSV-G
SARS-S
SARS-2-S
Pseudotype Entry [x-fold over Background]
A549
BEAS-2B
Calu-3
H1299
MRC-5
293T
Huh-7
Caco-2
Vero
LLC-PK1
MDBK
MDCK II
RhiLu/1.1
MyDauLu/47.1
BHK-21
NIH/3T3

Figure 2

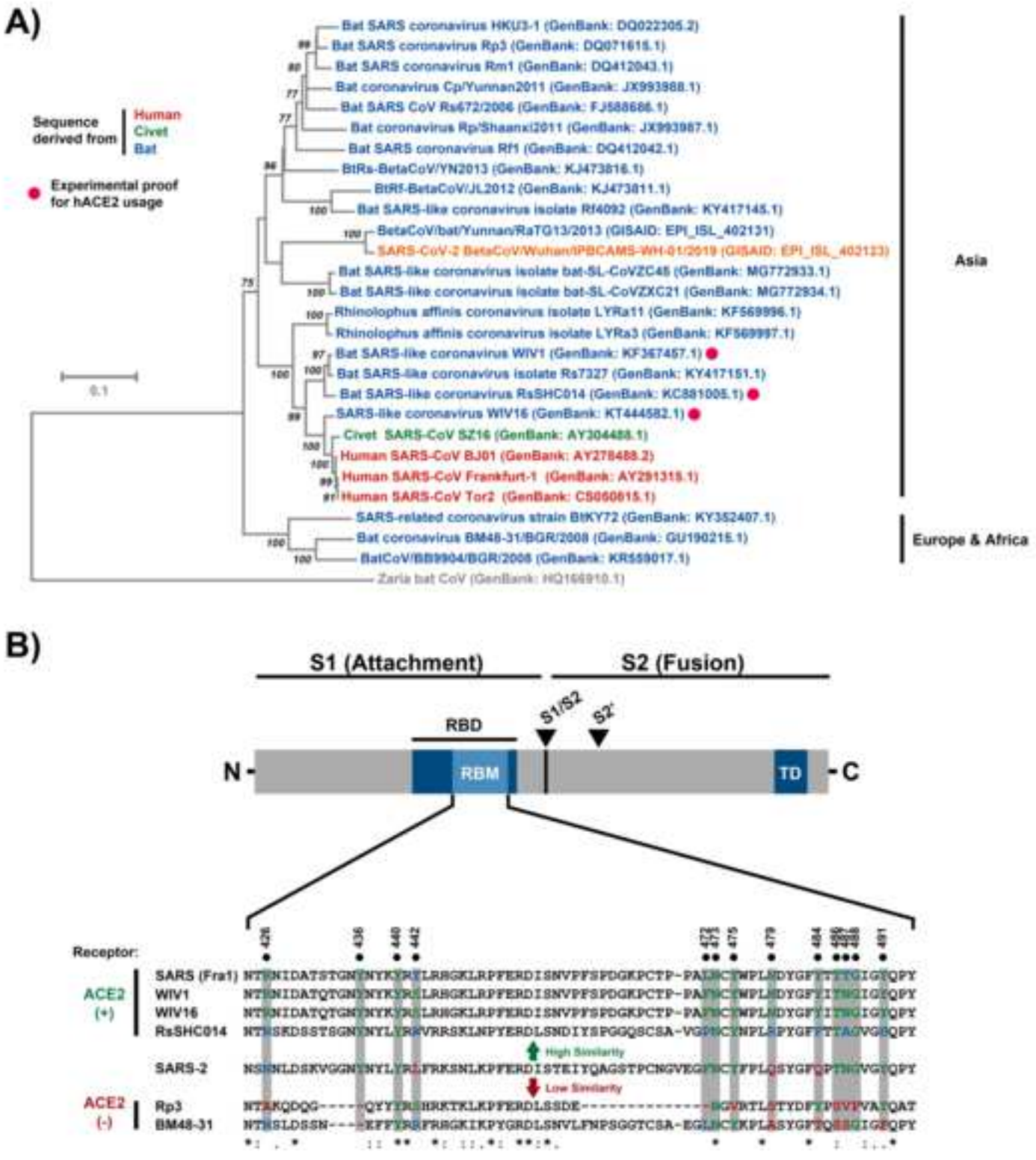
A)
Sequence derived from
Human
Civet
Bat
Experimental proof for hACE2 usage
0.1
Bat SARS coronavirus HKU3-1 (GenBank: DQ022305.2)
Bat SARS coronavirus Rp3 (GenBank: DQ071615.1)
Bat SARS coronavirus Rm1 (GenBank: DQ412043.1)
Bat coronavirus Cp/Yunnan2011 (GenBank: JX993988.1)
Bat SARS CoV Rs672/2006 (GenBank: FJ588686.1)
Bat coronavirus Rp/Shaanxi2011 (GenBank: JX993987.1)
Bat SARS coronavirus Rf1 (GenBank: DQ412042.1)
BtRs-BetaCoV/YN2013 (GenBank: KJ473816.1)
BtRf-BetaCoV/JL2012 (GenBank: KJ473811.1)
Bat SARS-like coronavirus isolate Rf4092 (GenBank: KY417145.1)
BetaCoV/bat/Yunnan/RaTG13/2013 (GISAID: EPI_ISL_402131)
SARS-CoV-2 BetaCoV/Wuhan/IPBCAMS-WH-01/2019 (GISAID: EPI_ISL_402123)
Bat SARS-like coronavirus isolate bat-SL-CoVZC45 (GenBank: MG772933.1)
Bat SARS-like coronavirus isolate bat-SL-CoVZXC21 (GenBank: MG772934.1)
Rhinolophus affinis coronavirus isolate LYRa11 (GenBank: KF569996.1)
Rhinolophus affinis coronavirus isolate LYRa3 (GenBank: KF569997.1)
Bat SARS-like coronavirus WIV1 (GenBank: KF367457.1)
Bat SARS-like coronavirus isolate Rs7327 (GenBank: KY417151.1)
Bat SARS-like coronavirus RsSHC014 (GenBank: KC881005.1)
SARS-like coronavirus WIV16 (GenBank: KT444582.1)
Civet SARS-CoV SZ16 (GenBank: AY304488.1)
Human SARS-CoV BJ01 (GenBank: AY278488.2)
Human SARS-CoV Frankfurt-1 (GenBank: AY291315.1)
Human SARS-CoV Tor2 (GenBank: CS000815.1)
SARS-related coronavirus strain BtKY72 (GenBank: KY352407.1)
Bat coronavirus BM48-31/BGR/2008 (GenBank: GU190215.1)
BatCoV/BB9904/BGR/2008 (GenBank: KR559017.1)
Zaria bat CoV (GenBank: HQ166910.1)
Asia
Europe & Africa
B)
S1 (Attachment)
S2 (Fusion)
RBD
S1/S2
S2'
N
RBM
TD
C
Receptor:
ACE2 (+)
SARS (Fra1)
WIV1
WIV16
RsSHC014
SARS-2
High Similarity
Low Similarity
ACE2 (-)
Rp3
BM48-31

Figure 3

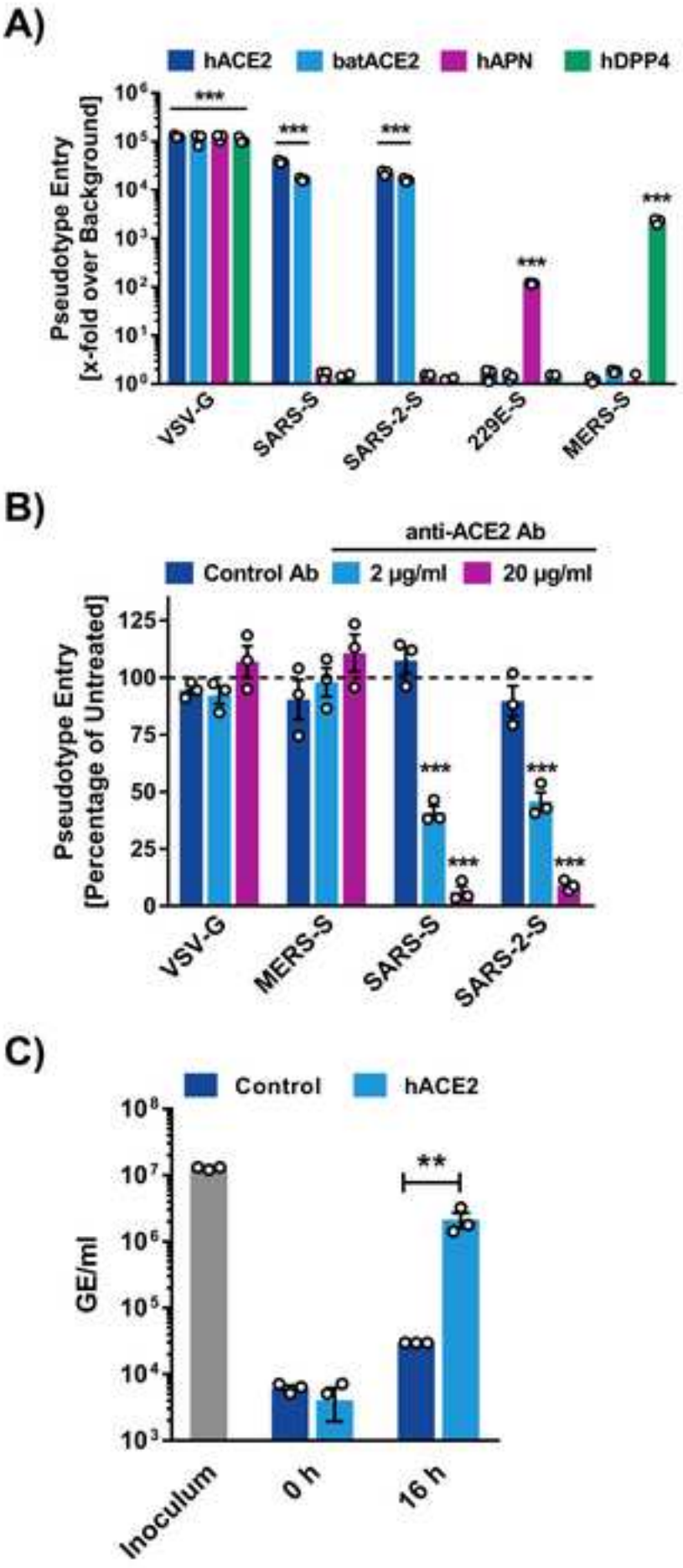
A)
hACE2
batACE2
hAPN
hDPP4
Pseudotype Entry
[x-fold over Background]
VSV-G
SARS-S
SARS-2-S
229E-S
MERS-S
B)
anti-ACE2 Ab
Control Ab
2 µg/ml
20 µg/ml
Pseudotype Entry
[Percentage of Untreated]
VSV-G
MERS-S
SARS-S
SARS-2-S
C)
Control
hACE2
GE/ml
Inoculum
0 h
16 h

Figure 4

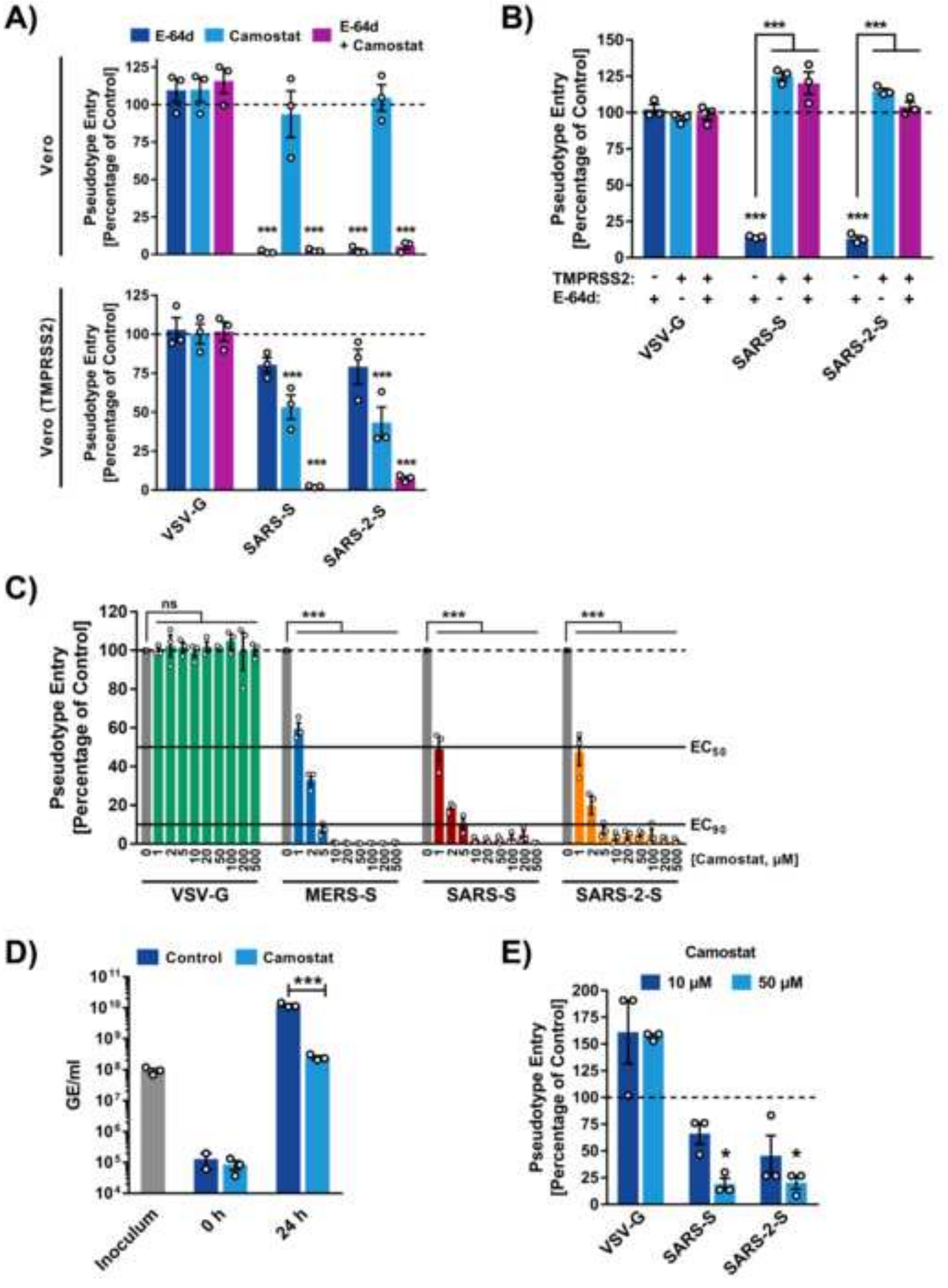
A)
E-64d
Camostat
E-64d + Camostat
Vero
Vero (TMPRSS2)
Pseudotype Entry [Percentage of Control]
VSV-G
SARS-S
SARS-2-S
B)
TMPRSS2:
E-64d:
C)
ns
VSV-G
MERS-S
SARS-S
SARS-2-S
[Camostat, μM]
D)
Control
Camostat
GE/ml
Inoculum
0 h
24 h
E)
Camostat
10 μM
50 μM

Figure 5

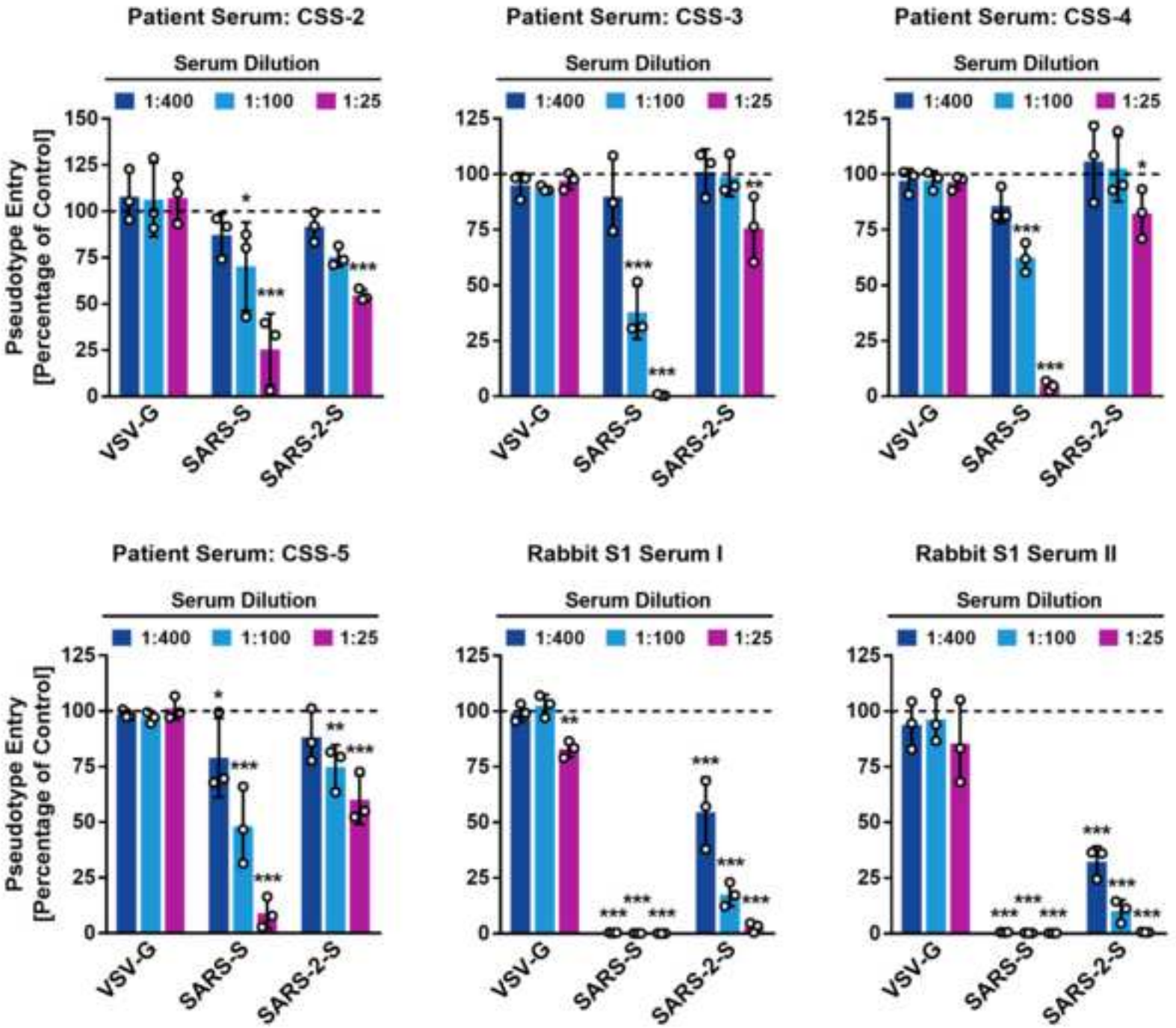
Patient Serum: CSS-2
Patient Serum: CSS-3
Patient Serum: CSS-4
Patient Serum: CSS-5
Rabbit S1 Serum I
Rabbit S1 Serum II
Serum Dilution
1:400
1:100
1:25
Pseudotype Entry [Percentage of Control]
VSV-G
SARS-S
SARS-2-S

Supplemental Figure 1

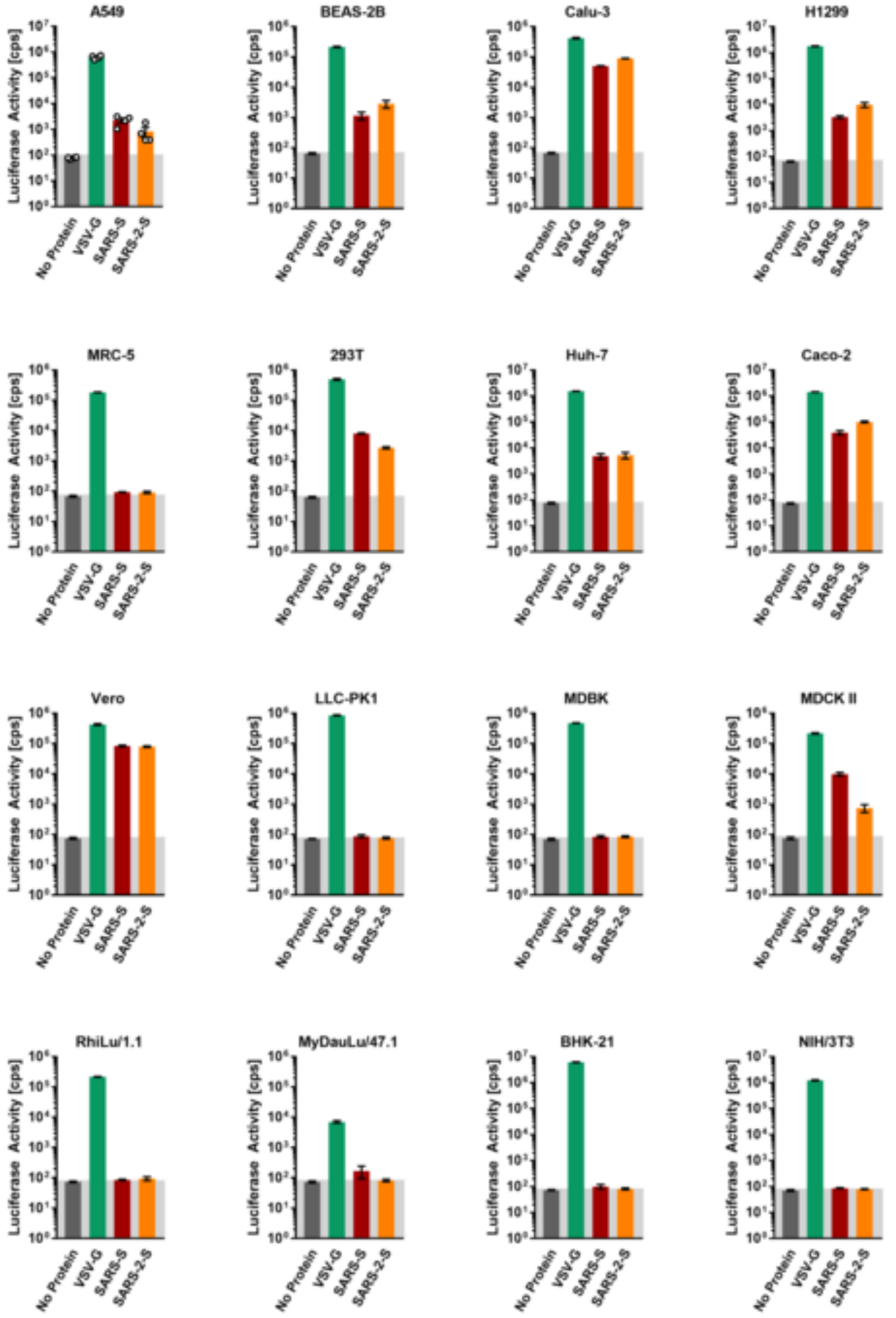

Supplemental Figure 2

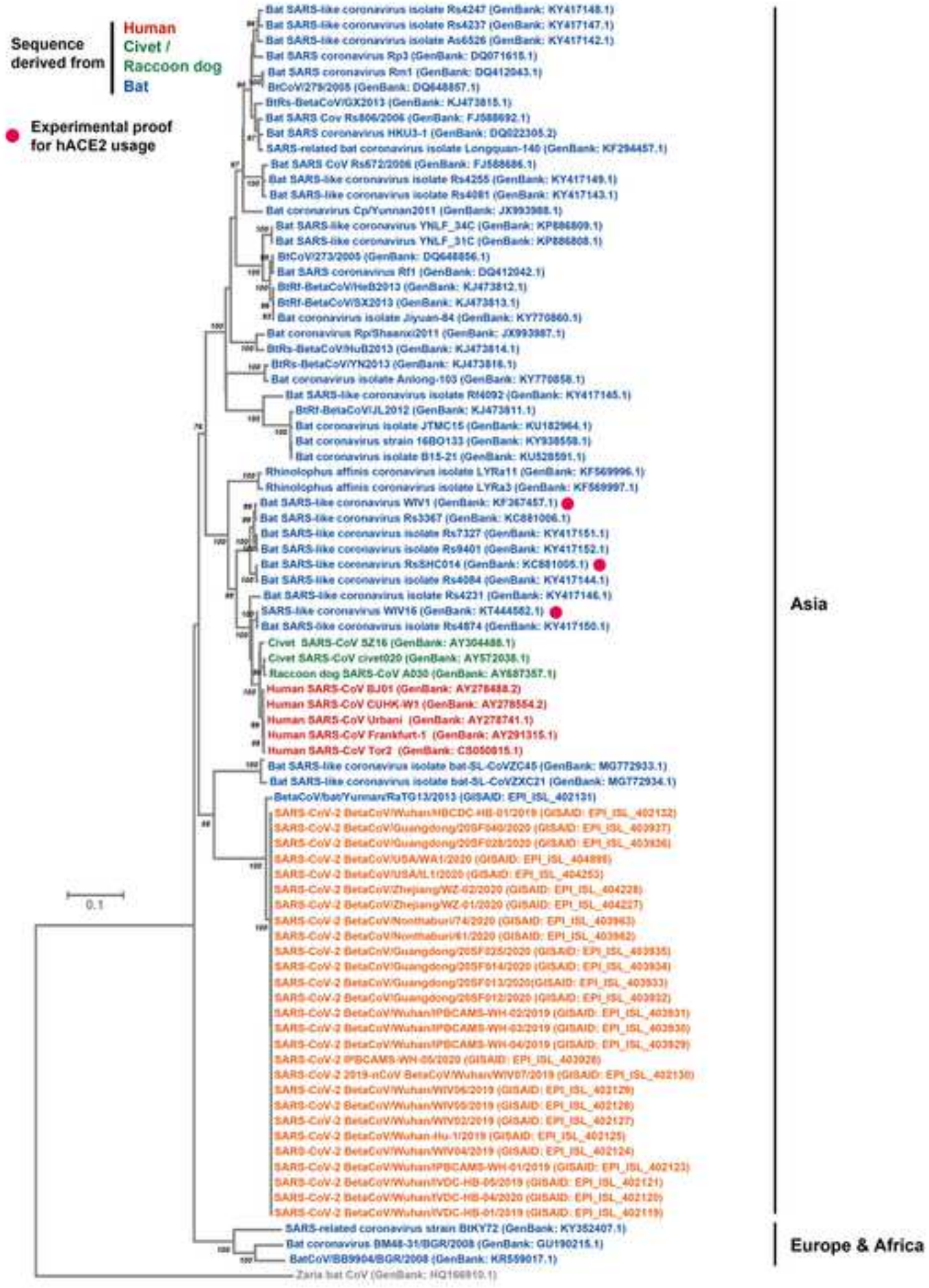

Supplemental Figure 3